Journal of Soils and Sediments (2022) 22:134–145
https://doi.org/10.1007/s11368-021-03050-6

SOILS, SEC 3 • REMEDIATION AND MANAGEMENT OF CONTAMINATED OR DEGRADED LANDS • RESEARCH ARTICLE

Characteristics of PAHs in soils under different land-use types and their associated health risks in the northern Taihu Basin, China

Tian Sun[1] · Yanhua Wang[1,2,3] · Jiaming Tian[1] · Xinggong Kong[1]

Received: 24 March 2021 / Accepted: 5 August 2021 / Published online: 8 September 2021

Abstract

Purpose Polycyclic aromatic hydrocarbons (PAHs) in the environment are strongly influenced by anthropogenic activities and negatively impact human health. Identifying the sources and potential risks of PAHs in soils will help to prevent soil pollution and utilize land more effectively.

Materials and methods In this study, soils under different land-use types in the northern Taihu Basin were investigated. The PAHs in soils were measured by gas chromatography-mass spectrometry. The toxicity of PAHs from different sources was quantitatively evaluated based on the positive matrix factorization-toxic equivalent quantity (PMF-TEQ) model. The incremental lifetime cancer risk (ILCR) method was used to assess the health risk of PAHs.

Results and discussion The results showed that the Σ_{16}PAHs concentrations varied between 142.26 and 9278.51 ng g^{-1}, with a mean value of 1640.43 ng g^{-1}. High molecular weight PAHs were found to account for the largest fractions (87%) of the Σ_{16}PAHs. Significant variation of the PAHs concentrations in soils was observed under different land-use types. The mean concentration of Σ_{16}PAHs in different areas was in the order of industrial area > traffic area > commercial area > residential area > park > farmland. Vehicle emissions and coal/coke combustion were the predominant sources, accounting for 54% and 37% of the Σ_{16}PAHs loading, respectively. The total predicted TEQ of PAHs ranged from 15.71 to 867.35 ng g^{-1} (mean 189.29 ng g^{-1}), and benzo(a)pyrene was the major species. The total ILCR value for soil PAHs exposure was in a range of $(0.13 \sim 9.13) \times 10^{-6}$.

Conclusions Source identification showed that the dominant source of soil PAHs was vehicle emissions in commercial (89%) and traffic (85%) area, while coal/coke combustion was the main source of soil PAHs in industrial area (43%). The total TEQ indicated a potential carcinogenic risk in the study area, with vehicle emissions and coal/coke combustion making the primary contribution to the total TEQ (95%). The total ILCR value was in a range of $10^{-7} \sim 10^{-5}$, which indicated a low health risk. Children experienced a higher cancer risk than adults due to their sensitivity to the carcinogenic effects of PAHs.

Keywords PAHs · Land-use type · Soil · Health risks · Taihu Basin

1 Introduction

Polycyclic aromatic hydrocarbons (PAHs) are ubiquitous environmental contaminants due to their carcinogenic, immunotoxic, and mutagenic effects on organisms (Wu et al. 2014; Obrist et al. 2015; Lei et al. 2016; Balgobin and Singh 2019 and references therein). With the increase in benzene ring number, PAHs with a high molecular weight becomes more stable and have stronger toxicity. These PAHs can resist biodegradation and persist in the environment for a long time. The environmental behavior of PAHs has become a cause for concern (Wu et al. 2014; Lei et al. 2016; Balgobin and Singh 2019). PAHs are mainly derived from

Responsible editor: Zhaohui Wang

✉ Yanhua Wang
wangyanhua@njnu.edu.cn

[1] School of Geography, Nanjing Normal University, 1 Wenyuan Road, Nanjing 210023, Qixia, China

[2] Jiangsu Center for Collaborative Innovation in Geographical Information Resource Development and Application, Nanjing, China

[3] Key Laboratory of Virtual Geographic Environment (Nanjing Normal University), Ministry of Education, Nanjing 210023, China

the burning of various organic materials, including natural sources, i.e., volcanic eruptions and forest fires, as well as anthropogenic activities such as vehicle emissions, coal combustion, and oil leakage (Li et al. 2019a; Parra et al. 2019). Different sources of PAHs may exhibit various levels of toxicity due to the different dominance of ring numbers. Therefore, it is crucial to clarify the toxicity of PAHs from different sources before developing cost-effective abatement strategies (Yin et al. 2015; Zheng et al. 2018; He et al. 2020).

Soil serves as a "sink" for PAHs in the environment, which can become tightly bound to soil particles following atmospheric deposition and sewage irrigation due to their high hydrophobicity (Cetin 2016; Zheng et al. 2018). The enrichment of PAHs in soils can eventually affect human health through the food chain or various other exposure routes (Lemieux et al. 2015; Qi et al. 2019; Wang et al. 2020a; Xu et al. 2021). The PAHs concentrations in soils reflect the environmental quality (Qi et al. 2019), and their distribution in the soil can be used to assess pollution levels (Jia et al. 2017), identify emission sources (Lu et al. 2020), and evaluate the environmental health risks associated with PAHs (Zheng et al. 2018).

In recent decades, the emission of PAHs in China has been on the rise (Xu et al. 2006; Mu XL 2016) accompanied by an increasing proportion of high-molecular weight PAHs (Zhang et al. 2011). PAHs have become major contaminants in urban soils and pose potential carcinogenic risks to urban residents (Zheng et al. 2018; Chen and Liang 2021), especially in areas with a high population density and high level of anthropogenic activities (Xu et al. 2021). The northern Taihu Basin is such a region, located in the Yangtze River Delta in China. In this century, the environment of the northern Taihu Basin has been deteriorated to be a heavily polluted area as a result of intense anthropogenic activities (Chen et al. 2020; Huang et al. 2020; Li et al. 2020a). Most of the current studies focused on the algae bloom, changes in nitrogen and phosphorus contents, sediment thickness and dredging, and effects of multiple factors, i.e., wind-wave disturbance, temperature, dissolved oxygen, and pH value on the lake water quality (Zheng et al. 2015; Zhong et al. 2020; Chen et al. 2021). The non-point pollution from agriculture has also been paid more attention to (Chen et al. 2020) in the Taihu Basin. With the economic development, the intensity and patterns of anthropogenic activity varied within the different land-use types, resulting in differences in soil contamination between different regions (Peng et al. 2011; Jia et al. 2017; Li et al. 2020a). However, at present, limited researches on the persistent organic pollutants, especially PAHs in soils from different functional areas of the basin, and the cancer risks of human exposure to PAHs. The objectives of this study were as follows: (1) to investigate the concentrations and sources of PAHs in soils under different land-use types in the northern Taihu Basin, (2) to quantitatively estimate the toxicity of PAHs from various sources, and (3) to evaluate the incremental lifetime cancer risk (ILCR) due to exposure to PAHs in soils. It is expected that our study will provide a scientific basis for soil remediation and human health risk management.

2 Materials and methods

2.1 Study area and sampling

Taihu Lake is the third-largest freshwater lake in China, with approximately 120 inflows and outflows around the lake. The inflows are mainly located in the northern and western parts of the lake (Li et al. 2019b). Wuxi City is located in the northern part of the Taihu Basin and has more than 6 million inhabitants. In the "13th Five-Year Plan," the government proposed to develop Wuxi City into a national integrated transport hub. The total number of vehicles in Wuxi City reached 2.02 million in 2018, which represented an increase of 1.73 times compared to that in 2000. The raw coal, coke, and crude oil consumption of major industrial enterprises in this region reached 25.68, 4.33, and 1.37 million tons, respectively in 2018, which represented an increase of 1.51, 54.72, and 3.75 times compared to the values in 2000, respectively (Wuxi City Bureau of Statistics 2000–2018). Large volumes of treated industrial effluents from the city are discharged into the northern part of Taihu Lake via the Wangyu River (Lei et al. 2016). The total nitrogen (TN) and total phosphorus (TP) concentrations allowed by the national Level A discharged standard are 15 and 0.5 mg L^{-1}, respectively, and the allowable discharged concentrations of other pollutants are also high (Environmental Protection Department of Jiangsu Province 2007).

In August 2020, a total of 14 representative topsoil samples (0 ~ 10 cm) in different areas were collected from the northern Taihu Basin (mainly the Binhu District of Wuxi City). The sample sites represented various land-use types, covering industrial areas (I1, I2, and I3), a commercial area (C1), traffic areas (T1 and T2), residential areas (R1, R2, R3, and R4), parks (P1, P2), and farmland (A1 and A2). The distribution of each sampling site is shown in Fig. 1. A stainless steel shovel was used to collect the 0 ~ 10-cm surface samples at each site. Artificial fill was avoided, and all surface debris was removed. All samples were stored in well-labeled sealed bags at –20 °C for subsequent processing and analysis.

2.2 Sample preparation and instrument analysis

Impurities (i.e., stones, plants, and animal residues) were removed from freeze-dried samples. The samples were ground using an agate mortar and then passed through a 100

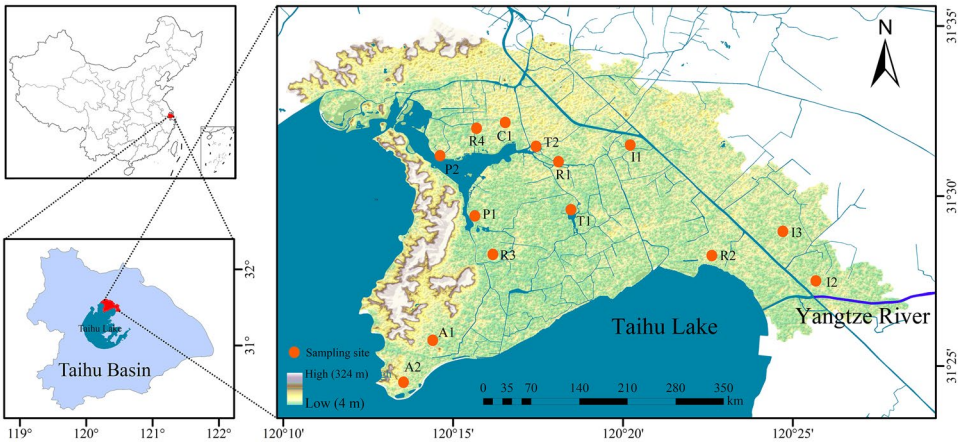

Fig. 1 Location of the sampling sites in the northern Taihu Basin

mesh sieve (particle size < 0.15 mm). Anhydrous sodium sulfate and silica gel were used as the column sorbent materials and were activated at 450 °C and 180 °C for 4 and 6 h, respectively, and were then allowed to cool to attain room temperature. Approximately 2 g (dry weight) of the sample was transferred into a 34-mL extraction cell and mixed with moderate diatomaceous earth for accelerated solvent extraction (ASE) using dichloromethane/hexane (1:1, v/v) as the solvent. The cell was placed into the carousel of an ASE 350 system (Thermo Scientific, USA). The system was filled with an *n*-hexane/dichloromethane mixture (1:1, v:v). The operating conditions were as follows: oven temperature of 100 °C, heating for 5 min, and static extraction for 5 min at a pressure of 1500 psi (10 MPa). The extract was collected from the sample cell with a 90-s nitrogen purge. The extract from the collection flask was transferred to a round bottom flask and concentrated to 2 mL through a vacuum rotary evaporation process in a 40 °C water bath. The extract was then transferred to the prepared chromatography column using a glass dropper. The clean-up column was filled from top to bottom with 1.5 g anhydrous sodium sulfate, 1 g silica gel, and 1.5 g anhydrous sodium sulfate. The purification column was then rinsed with a 15 mL *n*-hexane/dichloromethane mixture (1:1, v:v) and 5 mL *n*-hexane, and the solution was collected in a flask and decreased to 0.5 mL with an evaporator. The extract was transferred into a 2-mL vial. The *n*-hexane was used to rinse off the residual extract from the flask and diluted to exactly 1 mL with the solution (Chang et al. 2018; Chen and Liang 2021; Xia et al. 2021).

The pretreated samples were analyzed by a gas chromatography-mass spectrometer (GC–MS) system (Agilent 8860–5977, USA) with a DB-5MS (0.25-μm film thickness, 30 m × 0.25 mm i.d.) silica capillary column. High purity (99.999%) helium was used as the carrier gas at a constant flow rate of 1 mL min^{-1}. The injection volume was 1 μL of each sample, with a splitless injection method. The injector and detector temperatures were 250 and 280 °C, respectively. The initial temperature was 50 °C held for 1 min, ramped up to 180 °C at 15 °C min^{-1}, then to 280 °C at 5 °C min^{-1}, and subsequently maintained for 5 min. The mass detector was operated at 70 eV, and the temperature of the ion source was set to 280 °C. Sixteen PAHs were measured under the full scan mode (50 ~ 550 amu): 2 rings: naphthalene (Nap); 3 rings: acenaphthylene (Acy), acenaphthene (Ace), fluorene (Flu), phenanthrene (Phe), and anthracene (Ant); 4 rings: fluoranthene (Flua), pyrene (Pyr), benzo(a)anthracene (BaA), and chrysene (Chry); 5 rings: benzo(k)fluoranthene (BkF), benzo(b)fluoranthene (BbF), benzo(a)pyrene (BaP), and dibenzo(a,h)anthracene (DahA); and 6 rings: indeno(1,2,3-cd)pyrene (IcdP) and benzo(g,hi)perylene (BghiP).

2.3 Quality assurance and quality control

The glass bottles and round-bottomed flasks used in the experiment were baked at 500 °C for 4 h. A seven-point calibration curve (50, 100, 250, 500, 1000, 2000, and 2500 ng mL^{-1}) with a correlation coefficient ($r^2 > 0.996$) combined with an external standard method was applied to quantify PAHs. The target compounds were not detected in method blanks. The average recoveries of the sixteen PAHs in all samples were > 75%, and the resulting concentrations were not corrected with recoveries. The relative standard deviations of the sixteen PAHs in the duplicate samples were all less than 10%, and the PAH concentrations in this study were based on dry-weight soil samples.

2.4 Source quantification and toxicity evaluation of PAHs

2.4.1 The positive matrix factorization model

The PMF model was applied to quantitatively determine the source profiles of PAHs in soils. This model was first proposed by Paatero and Tapper (1994). The uncertainty of the variables was taken into account and all values were

positive. The model did not require source profile data. It was therefore particularly suitable for identifying and quantifying source profiles and the contributions of PAHs in the environment (i.e., urban air, soils, and lake sediments) (Li et al. 2016; Yang et al. 2018). The PMF model is commonly used as a quantitative source resolution method. The model can be described by Eq. (1):

$$E_{ij} = \sum_{k=1}^{p} A_{ik} B_{kj} + \varepsilon_{ij} \quad (1)$$

where i represents the detected sample, j refers to the PAHs species, p refers to the number of source factors, B is the component matrix of each source, A represents the contribution matrix of each contaminant, and ε_{ij} refers to the random error.

$$Q = \sum_{i=1}^{n} \sum_{j=1}^{m} \left(\frac{\varepsilon_{ij}}{\sigma_{ij}} \right)^2 \quad (2)$$

where Q refers to the weighted sum of squares for the difference between the PMF output and the original dataset and σ_{ij} represents the uncertainty in the j_{th} PAHs for sample i. The details of the uncertainty are provided by Yang et al. (2021). All of the values of the uncertainty file are needed to calculate the confidence level of the model. The concentration and uncertainty file for each value should be positive. Consequently, the concentrations of individual PAHs in soil samples were replaced by half of its method-detection-limit (MDL) if they were below the corresponding MDL value.

2.4.2 Risk assessment

The toxicity equivalency factor (TEF) method was applied to calculate the toxic concentrations of PAHs in soil samples. The most widely studied carcinogenic PAHs, BaP, was selected as a reference species for the toxicity assessment. Subsequently, BaP-based TEFs were used to evaluate the toxicity of the different sources identified by the PMF model and the predicted PAHs concentration from each source. The TEF value was calculated as follows:

$$\text{TEQ}^{ik} = \sum\nolimits_{j=1}^{m} \text{C}_j^{ik} \cdot \text{TEF}_j \quad (3)$$

where TEQ^{ik} indicates the total toxic equivalent quantity (TEQ) of factor k from sample i, c_j^{ik} represents the predicted concentration of species j emitted by source k in sample i, and TEF_j is the TEF of species j from the literature (Nisbet and Lagoy 1992; Samburova et al. 2017).

The ILCR method was used to quantify the potential health risk of PAHs in soils to children and adults (Chen and Liang 2021). The ILCR value for soil PAHs was calculated according to Eqs. (4) to (7). The relevant exposure pathways of soil PAHs throughout a human lifetime include direct ingestion, dermal absorption, and inhalation (Table S1).

$$\text{ILCR}_{Ing} = \frac{C_{soil} \times \left(\text{CSF}_{Ing} \times \sqrt[3]{\text{BW}/70} \right) \times \text{IR}_{Ing} \times \text{EF} \times \text{ED}}{\text{BW} \times \text{AT}\times} \quad (4)$$

$$\text{ILCR}_{Der} = \frac{C_{soil} \times \left(\text{CSR}_{Der} \times \sqrt[3]{\text{BW}/70} \right) \times \text{SA} \times \text{AF} \times \text{ABS} \times \text{EF} \times \text{ED}}{\text{BW} \times \text{AT} \times 10^6} \quad (5)$$

$$\text{ILCR}_{Inh} = \frac{C_{soil} \times \left(\text{CSR}_{Inh} \times \sqrt[3]{\text{BW}/70} \right) \times \text{IR}_{Inh} \times \text{EF} \times \text{ED}}{\text{BW} \times \text{AT} \times \text{PEF}} \quad (6)$$

$$\text{ILCR}_{tot} = \text{ILCR}_{Ing} + \text{ILCR}_{Der} + \text{ILCR}_{Inh} \quad (7)$$

where ILCR_{Ing}, ILCR_{Der}, and ILCR_{Inh} represent the cancer risks associated with the exposure pathways via ingestion, dermal contact, and inhalation, respectively, and ILCR_{tot} is the total cancer risk. More of the parameters referred to in the equations are presented in Table S1 (Yang et al. 2015). The qualitative descriptions of the ILCR were as follows: acceptable health risk ($\leq 10^{-6}$), low health risk ($10^{-6} \sim 10^{-4}$), moderate health risk ($10^{-4} \sim 10^{-3}$), high health risk ($10^{-3} \sim 10^{-1}$), and very high health risk ($\geq 10^{-1}$) (Qi et al. 2019).

2.5 Statistical analysis

All statistical tests were performed with the statistical program SPSS 21.0 (SPSS Inc. Chicago, USA). A *T*-test was applied to compare the PAHs levels in soils from the areas with different land-use types. For a principal component analysis (PCA), all socio-economic parameters were log-transformed to obtain a normal distribution of data. An eigenvalue over 1 was selected to explain the percentage of the total variation attributed to each parameter based on the Kaiser criterion. A linear regression of the PAHs in soils versus the derived principal components was then conducted. Statistical significance was verified by an *F*-test of the overall fit, followed by a *T*-test for each parameter. The data for the socio-economic parameters used in the PCA were obtained from http://www.tianditu.gov.cn/.

3 Results and discussion

3.1 Characteristics of PAHs concentrations in soils

The Σ_{16}PAHs concentration in soils of the different land-use types in the northern Taihu Basin is shown in Fig. 2, with a mean value of 1640.43 ng g^{-1} (range of 142.26 ~ 9278.51 ng g^{-1}). The classification criteria for PAHs contaminated soils according to

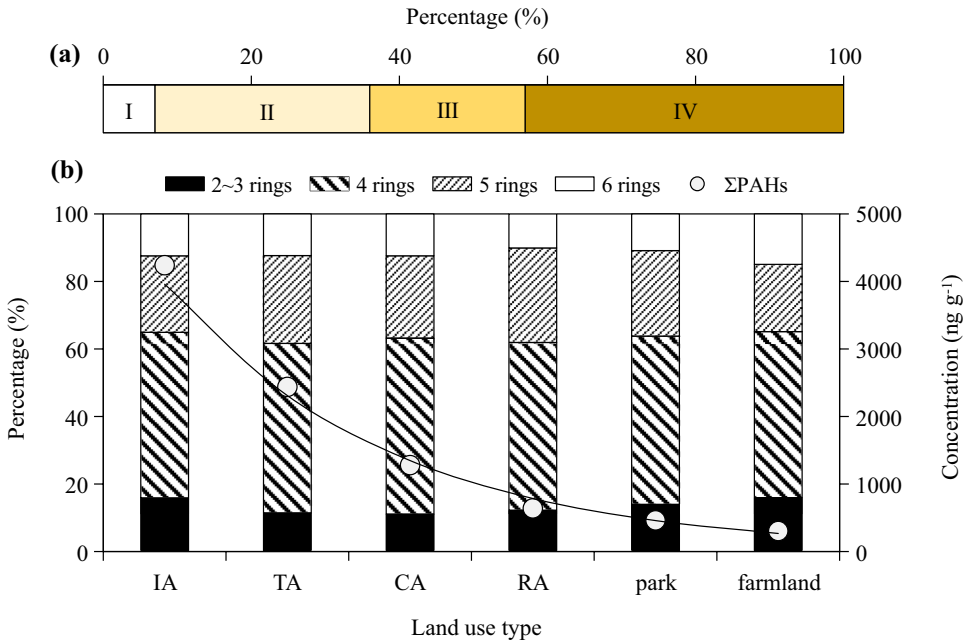

Fig. 2 The percentage of each pollution grade (**a**), and distributions of Σ_{16}PAHs (**b**) summarized by the ring number in soil samples from different areas. (I) Bon-contaminated soil; (II) weakly contaminated soil; (III) contaminated soil; (IV) heavily contaminated soil; IA industrial area, TA traffic area, CA commercial area, RA residential area

the standard proposed by Maliszewska-Kordybach (1996) were used as a reference, with the result that 7%, 29%, 21%, and 43% of the sampling sites corresponded to non-contaminated soil (< 200 ng g^{-1}), weakly contaminated soil (200 ~ 600 ng g^{-1}), contaminated soil (600 ~ 1000 ng g^{-1}), and heavily contaminated soil (> 1000 ng g^{-1}), respectively. The concentrations of some individual PAHs in samples from industrial, traffic, and commercial area exceeded the Chinese Agricultural Soil Environmental Quality Standard (China's Ministry of Environmental Protection 2009). Of the sixteen PAHs, BbF (43%), Chry (36%), BaA (21%), and IcdP (21%) had the highest exceedance rates, indicating a large potential risk. Based on this standard, the most contaminated soil sample was found at site I1, which was an industrial area, where the concentrations of Phe, Ant, Flua, Pyr, BaA, Chry, BbF, BkF, BaP, DahA, and IcdP in soils exceeded their environmental quality standards, followed by sites I2 and T1, where the concentrations of BaA, Chry, BbF, and IcdP in soils exceeded the standard. The main species that exceed the standard were high molecular weight PAHs (HPAHs), i.e., including 4 ~ 6 rings. The Σ_{16}PAHs concentration in soils from the northern Taihu Basin was high in comparison to reported values in soils from South Korea (23.3 ~ 2834 ng g^{-1}) (Nam et al. 2003) and underdeveloped western China (141 ~ 191 ng g^{-1}) (Sun et al. 2017), and was comparable to the values reported in Tianjin (58.2 ~ 9160 ng g^{-1}) and Zhengzhou (49.9 ~ 11,565 ng g^{-1}) in China. Compared to other soils, i.e., Shanghai (251 ~ 18,916 ng g^{-1}) (Chen and Liang 2021) in China, Tampa (59 ~ 58,640 ng g^{-1}), and Orlando (43 ~ 30,428 ng g^{-1}) in the USA (Liu et al. 2019), the PAHs concentration in soils investigated in this study was lower.

The result of the *T*-test revealed that the Σ_{16}PAHs concentrations in soils from different land-use types varied significantly ($p < 0.05$), with the concentrations in soils from industrial and traffic area being much higher than those from areas with other land-use types. The mean Σ_{16}PAHs concentration in soils followed the descending order of: industrial area (4240.80 ng g^{-1}) > traffic area (2433.13 ng g^{-1}) > commercial area (1280.07 ng g^{-1}) > residential area (638.94 ng g^{-1}) > park (461.68 ng g^{-1}) > farmland (304.06 ng g^{-1}). The large volume of fossil fuels consumed in the industrial area could lead to an accumulation of PAHs in the environment. In particular, the oil processing plant at site I1 was responsible for contamination from petroleum hydrocarbons due to waste oil discharges and leakages (Zong et al. 2019). The frequent use of large trucks for transport, as well as the stop-start motion of trucks in transit releases exhaust gases rich in PAHs (Yang et al. 2021). High traffic volumes in traffic area lead to large amounts of diesel and petrol combustion, which increases PAHs level in the environment.

There were slight differences in PAH composition patterns among the different land-use areas (Fig. 2). The PAHs composition in soils was dominated by 4 ~ 5 rings, attributing 43 ~ 58% (mean 50%) and 15 ~ 31% (mean 25%) of the Σ_{16}PAHs, respectively. The most abundant PAHs were the HPAHs (mean 87%), with low molecular weight PAHs (LPAHs) (2 ~ 3 rings) accounting for less than 20%. This might be related to the different vapor pressures of individual PAHs. Due to their relatively high vapor, LPAHs are more volatile than HPAHs. They are therefore effectively distilled and transported, whereas HPAHs tend to remain near the emission source due to their large sorption capacity and resistance to degradation (Li et al. 2020b). Previous studies have shown that the high-temperature combustion

of organic materials for industrial production emits large amounts of HPAHs, while low-temperature combustion of organic matter for domestic heating or in small workshops releases a higher proportion of LPAHs (Hadibarata et al. 2019). The predominance of HPAHs in the soil samples reflected a developed industrial civilization, which was consistent with the social development level of the study area in the "economic center of the Yangtze River Delta." There were similar composition patterns of PAHs among the various land-use areas, suggesting homology of PAHs in soils. Only the proportion of LPAHs in soils varied, with the levels in industrial area and farmland being slightly higher than the levels in soils from other land-use types. This was attributed to oil leakage during production in industrial area and the combustion of biomass or civilian coal in farmland.

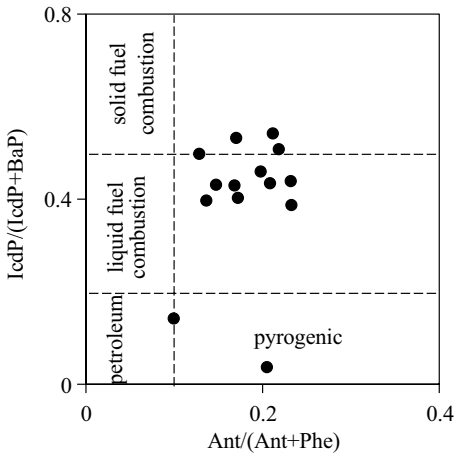

Fig. 3 Diagnostic ratios of Ant/(Ant + Phe) and IcdP/(IcdP + BaP) based on the use of PAHs isomers for source identification in soils

3.2 The sources of PAHs and associated influencing factors

3.2.1 Source apportionment

Due to the fingerprinting potential of PAHs in different emissions, some specific PAHs (i.e., Phe and BghiP) are often used as indicators of specific formation processes, and their ratios can suggest different emission sources. The diagnostic ratios of PAHs isomers are widely used for the tracing of potential PAHs' sources (Wang et al. 2011; Zheng et al. 2020). The diagnostic ratios of Ant/(Ant + Phe) and IcdP/(IcdP + BghiP) have been used to characterize their potential sources (Dashtbozorg et al. 2019; Yang et al. 2019). In this study, the diagnostic ratios of Ant/(Ant + Phe) and IcdP/(IcdP + BghiP) were found to have ranges of 0.10 ~ 0.23 and 0.04 ~ 0.54, respectively (Fig. 3). It has been reported that Ant/(Ant + Phe) ratios below 0.1 suggest a petroleum source, whereas values above 0.1 are associated with pyrogenic sources. All samples had Ant/(Ant + Phe) ratios greater than 0.1, indicating that PAHs in soils were mainly derived from the burning of various substances. IcdP/(IcdP + BghiP) ratios < 0.2 indicate a petroleum source, while values between 0.2 and 0.5 indicate the burning of liquid fossil fuel, and values above 0.5 indicate solid fuel combustion (i.e., biomass, wood, and coal). About 86% of the samples presented IcdP/(IcdP + BaP) ratios > 0.2, of which 57% fell with the range from 0.2 to 0.5, and the IcdP/(IcdP + BaP) ratios for 29% of the samples were above 0.5, indicating a pyrogenic source for most of the PAHs in soils of the study area. The northern Taihu Basin is a developed urbanized and industrialized region, and industry is the main economic activity, which has also been boosted by the rapid growth of tourism with a large number of visitors in recent years. Therefore, energy consumption and transport usage have increased in this area (Zheng et al. 2020). We deduced that industrial development and transport were the main causes of the high PAHs concentration.

The mixing of various PAHs sources may produce average results that differ from their original characteristics, as shown in the literature (Semenov et al. 2017; Wang et al. 2020b), and variations in the transport of different isomers may also lead to a bias between diagnostic ratio results and reality (Katsoyiannis and Breivik 2014). Due to these issues, source apportionment methods may not work perfectly for determining diagnostic ratios. Consequently, the contributions of possible PAHs sources were separated and quantified by the PMF model. Four factors were extracted and their source profiles of PAHs are shown in Fig. 4. Factor 1 (F_1), accounting for 37% of the Σ_{16}PAHs, was dominated by Ace (90%), Ant (64%), Flu (60%), and Phe (53%). The burning of coal releases an abundance of LPAHs, and Ace, Flu, and Phe can be regarded as indicators of coke production (Li et al. 2018, 2020a). In addition, Ant and Phe are also used as tracers of coal combustion (Li et al. 2020a; Chen and Liang 2021). Many of the industrial enterprises in Wuxi City require large quantities of coal as an energy source, which is an important reason for the accumulation of PAHs in soils. Thus, F_1 was found to be a mixed source of coal and coke combustion, while F_2, which accounted for contributing 9% of Σ_{16}PAHs, had the highest NaP loading of 75%. It has been reported that NaP is present in large quantities in unburned petroleum (Zheng et al. 2017; Li et al. 2018; Zhang et al. 2019), and therefore, F_2 was considered to be the source representative of oil leakage. The F_3 factor explained 28% of Σ_{16}PAHs and was mainly loaded with BkF (55%) and IcdP (48%), both of which were identified as markers of diesel combustion (Zheng et al. 2017). Thus, F_3 was considered to represent the burning of diesel. The contribution of F_4 to the Σ_{16}PAHs was 26%, with the highest loadings from DahA

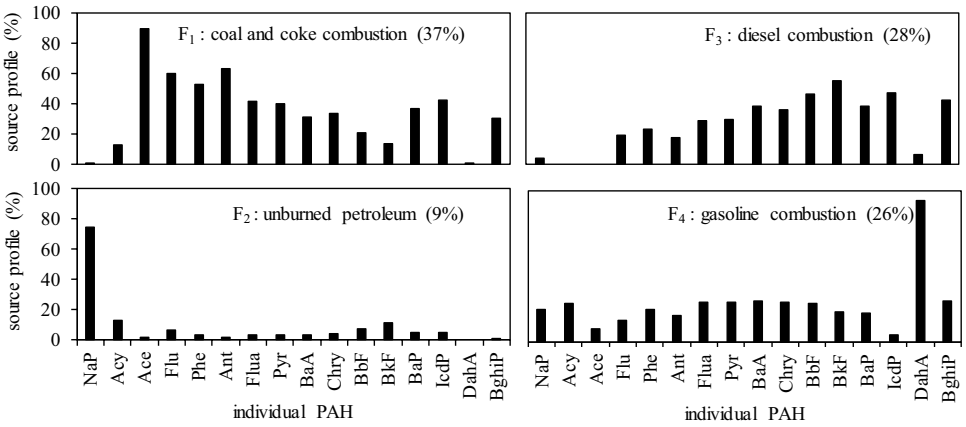

Fig. 4 Source profiles and quantitative contributions of PAHs in soils from the northern Taihu Basin based on the PMF model

(93%), which is a typical contaminant emitted from gasoline vehicles (Li et al. 2018), and consequently, F_4 was assigned to gasoline combustion. The accumulation of PAHs in soils from various pollution sources is a complex process, with vehicle emissions (diesel and gasoline combustion) contributing the most (54%) to the Σ_{16}PAHs concentration.

To further explore the mutual correlation between the PAHs concentration and socio-economic parameters, a PCA was performed (Table 1). The socio-economic parameters are presented in Table S2. Three principal components (PCs) were extracted to explain the percentage of the total variation among the parameters, with the three PCs explaining 83% of the total variation (Table 1). It was found that PC_1 was positively correlated with x_1, and made the largest contribution to the overall variance, while PC_2 was positively correlated with all parameters, with the values of x_3 and x_5 being statistically significant for PC_2. Finally, PC_3 was dominated by x_2, x_4, and x_6. There was a positive correlation between PC_1 and the Σ_{16}PAHs concentration, with a small coefficient in the model. Both PC_2 and PC_3 were negatively correlated with the Σ_{16}PAHs concentration, and a larger coefficient was observed, reflecting the major impact of PC_2 and PC_3 (transportation and industrial activities) on the Σ_{16}PAHs concentration in soils ($R = 0.5$; Table 2). The results showed that transportation, industrial activities, and green space had significant effects on the Σ_{16}PAHs concentration in soils. Therefore, we suggest increasing the area of woodland, which has a good absorption effect on PAHs, within the proximity of the main roads. Based on retaining the original ecosystem, forests have been planted around industrial point sources to isolate the pollution.

Table 1 Principal component analysis of the socio-economic parameters in the study area

Socio-economic parameter	Principal component (PC) for all data		
	PC_1	PC_2	PC_3
x_1	**0.32**	0.09	-0.30
x_2	0.16	0.47	**0.48**
x_3	-0.28	**0.45**	0.03
x_4	0.26	0.10	**0.52**
x_5	0.09	**0.51**	-0.57
x_6	-0.34	0.13	**0.18**
Pct. of var. (%)	42.00	23.34	17.77
Cum. pct. (%)	42.00	65.34	83.10

x_1, road width (km); x_2, distance from a sampling site to a road (km); x_3, distance from a sampling site to Wuxi railway station (km); x_4, distance from a sampling site to an industrial area within 1 km of it (km); x_5, size of the industrial area (km^2), x_6, size of a park within 1 km of a sampling site (km^2)

3.2.2 Emission sources in different land-use areas and the driving factors of PAHs pollution

The identification of PAHs sources in soils based on the PMF model was used to determine the PAHs concentration derived from different sources in the samples (Fig. 5). The PAHs derived from coal and coke combustion in soils ranged from 0.21 to 5897.29 ng g^{-1}, with a mean value of 623.32 ng g^{-1}. The highest concentrations of coal and coke combustion-derived PAHs were found at site I1 in the industrial area, with values in the remaining sites being < 500 ng g^{-1}. The PAHs originating from volatilization or the leakage of unburned petroleum were least abundant in soils, ranging from 184.76 to 1459.85 ng g^{-1}, with a mean value of 311.25 ng g^{-1}. The highest concentrations were observed at site I1 in the industrial area, which was associated with oil leakage during the production of oil products. Vehicle emissions-derived PAHs were found in soils with a range from 1.68 to 2951.50 ng g^{-1} and an average value of 825.57 ng g^{-1}. It should be noted that site T1 had the highest concentration of vehicle emissions-derived PAHs residues in soils. The cumulative contribution of each emission source to Σ_{16}PAHs differed under the different land-use types. Coal and coke combustion was the main

Table 2 Linear regression analysis of PAHs concentration vs. derived principal components and statistical significance

Equation	R	Significant level			
		F-test	T-test		
		F	$\|t_1\|$	$\|t_2\|$	$\|t_3\|$
$y = 0.01\ PC_1 - 0.40\ PC_2 - 0.43\ PC_3 + 4746.37 + \varepsilon$	0.5	0.96	0.03	0.74	1.41

y, Σ_{16}PAHs concentration; ε, residuals of the equation; $p < 0.1$

source of PAHs in soils from the industrial area, attributing 43% of the Σ_{16}PAHs predicted by the PMF model, with the highest contribution occurring at site I1 (64%). However, the primary source of Σ_{16}PAHs in soils was replaced by vehicle emissions in the commercial area (89%) and traffic area (85%), while its contribution to Σ_{16}PAHs in the residential area was also relatively high (51%). Unburned petroleum accounted for 55% and 49% of the Σ_{16}PAHs in soils from park and farmland, respectively. This might be related to that these two types of areas are relatively far from pollution sources, and the volatile PAHs derived from unburned petroleum are expected to be more effectively distilled and transported to these areas (Li et al. 2020b).

3.3 Toxicity assessment

A toxicity assessment of PAHs in soils from different sources was conducted through the application of the positive matrix factorization-toxic equivalent quantity (PMF-TEQ) model. The spatial variations of total TEQ from different sources identified by the PMF model are presented in Fig. 6a, and the toxicity profiles of each source are illustrated in Fig. 6b. The predicted total TEQ in soils from the study area ranged from 15.71 to 867.35 ng g^{-1}, with a mean value of 189.29 ng g^{-1}. The differences in the distribution of total TEQ displayed a similar pattern of variation to that of the Σ_{16}PAHs concentrations, with the TEQ in descending order by land-use type being industrial area (449.16 ng g^{-1}) > traffic area (308.75 ng g^{-1}) > commercial area (155.48 ng g^{-1}) > residential area (91.30 ng g^{-1}) > farmland (48.78 ng g^{-1}) > park (33.43 ng g^{-1}). The largest TEQ in soils was obtained from site I1 (867.35 ng g^{-1}). The samples exceeded the standard by 86%, suggesting a potential risk in the study area, especially in the industrial and traffic area where the toxicity was relatively high based on a reference value (32.96 ng g^{-1}) (Crnković et al. 2007).

For different sources, the contribution of coal and coke combustion, unburned petroleum, and vehicle emissions to Σ_{16}TEQ ranged from 15.15 to 36.50, 2.62 to 5.51 ng g^{-1}, and 60.44 to 82.22 ng g^{-1}, with mean values of 29.38, 4.49, and 66.13 ng g^{-1}, respectively. As shown in Fig. 6a, 95% of the total Σ_{16}PAHs toxicity was due to the contribution from pyrogenic sources, with coal and coke combustion explaining 34% and vehicle emissions explaining 61%. The toxicity profiles revealed the BaP was the dominant species, accounting for 67%, 62%, and 58% of the total toxicity from coal and coke combustion, unburned petroleum, and vehicle emission sources, respectively. This indicated that vehicle emissions were the primary source of PAHs toxicity in soils followed by urban industrial manufacturing, which was due to the intensity of anthropogenic activities in the study area.

To obtain a more accurate health risk assessment for human exposure to PAHs, the exposure pathways through direct ingestion, dermal contact, and inhalation were considered. Based on the total TEQ, the ILCR values for children and adults are summarized in Fig. 6c. The total cancer risk via dermal contact, ingestion, and inhalation for children and adults exposed to PAHs in soils was in a range of $(0.17 \sim 9.13) \times 10^{-6}$ and $(0.13 \sim 7.16) \times 10^{-6}$, respectively, indicating a potential carcinogenic risk. The total cancer risk of children exposed to soil PAHs was greater than that of adults, probably because children are

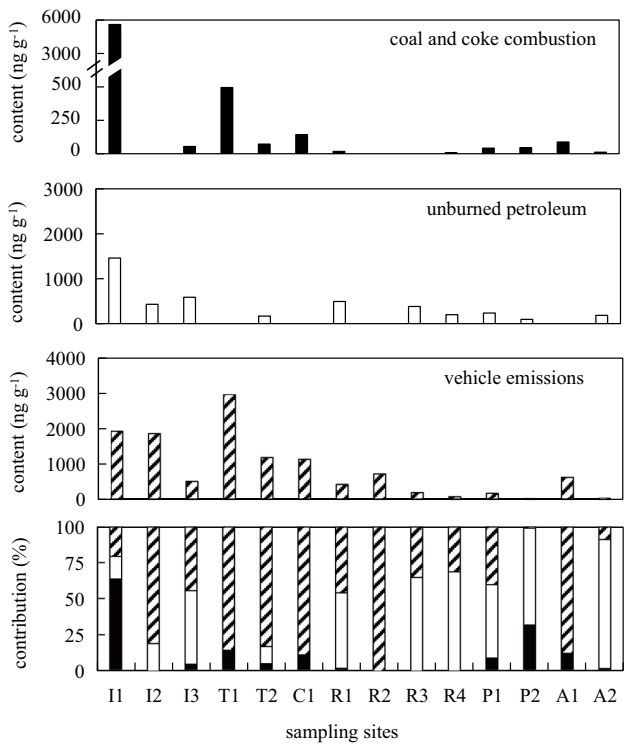

Fig. 5 Concentrations of PAHs from different sources in soil samples predicted by the PMF model

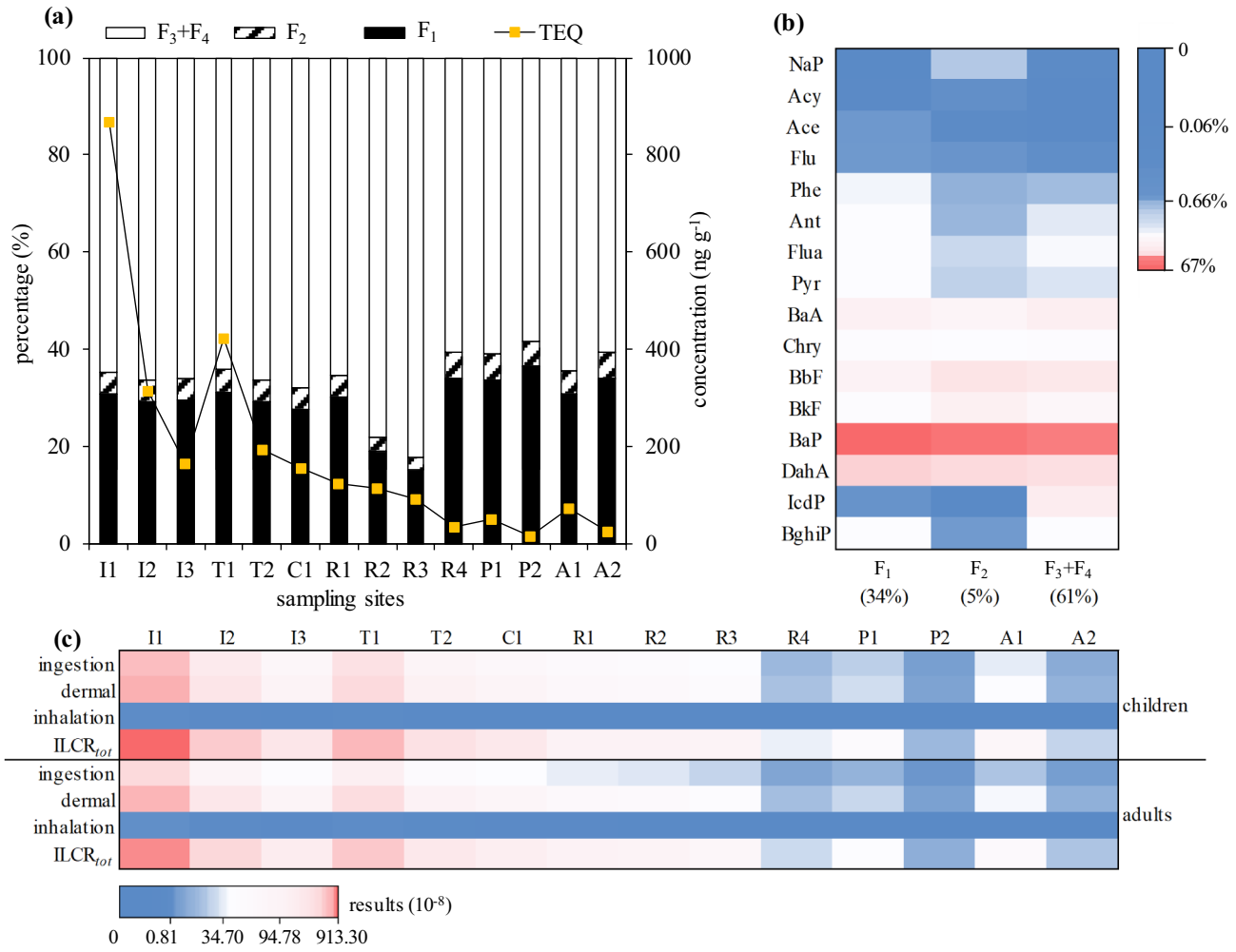

Fig. 6 The TEQ values from different sources in soils from various sites (**a**). The toxicity profiles based on the PMF model (**b**). The cancer risks for soil samples (**c**). Factors obtained by the PMF model were as follows, F_1: coal and coke combustion, F_2: unburned petroleum, F_3+F_4: vehicle emissions (diesel and gasoline combustion), $ILCR_{tot}$, the total cancer risk

more sensitive to the carcinogenic effects of PAHs, due to their underdeveloped immune systems. The ILCR values in the industrial, traffic, and commercial area ranged from 10^{-6} to 10^{-4}, which demonstrated that a low health risk would occur for human exposure to soil PAHs at these sites. If someone living or working near the industrial area or along the main road ingested, dermally contacted, or respired road dust, then the cancer risk would be higher. Except for these sites, the total cancer risk was equal to or less than the baseline of an acceptable health risk (10^{-6}).

The percentage concentrations of various exposure pathways to the total cancer risks are shown in Fig. S1. Dermal contact was the most important pathway, accounting for 54.45 ~ 65.10% of the total cancer risk. Compared with soil ingestion and dermal contact, human exposure to PAHs via the inhalation of resuspended particles from surface soils is limited. The inhalation of soil particles only accounted for 0.09 ~ 0.27% of the total cancer risk to human health. The inhalation of soil particles was therefore almost negligible when compared to other pathways. The same results have been reported elsewhere (Soltani et al. 2015; Yang et al. 2015).

In soil samples, the proportion of the total cancer risk from soil PAHs due to dermal contact for adults (65.10%) was higher than that for children (54.45%), which may be a consequence of adults having a higher dermal surface area and exposure duration than children. The proportion of the total cancer risk from the inhalation of soil particles was also greater for adults (0.27%) than for children (0.09%) due to the high inhalation rates of adults leading to more particulate matter entering the body through inhalation. Compared to dermal contact and the inhalation of soil particles, the cancer risk for adults generated by direct ingestion was lower than that for children, which could be explained by the fact that

children were the most sensitive subpopulation due to their frequent ingestion of contaminated dust via hand-to-mouth activities. The PAHs intake for children was also considered to be greater than that for adults due to their low body weight (Jia et al. 2017).

4 Conclusions

In this study, we focused on PAHs in soils of the northern Taihu Basin, China, to quantitatively estimate their spatial toxicities from different sources by applying the PMF-TEQ model. The highest PAHs concentration and toxicity were found in soils from industrial and traffic area, while the lowest values were found in soils from farmland and park. Three predominant PAHs sources, vehicle emissions (54%), coal and coke combustion (37%), and unburned petroleum (9%) were identified. Vehicle emissions (61%) made the primary contribution to the total toxicity. The ILCR values revealed that the cancer risk for children and adults from PAHs exposure in soils from industrial, traffic, and commercial area presented a low-risk, while the cancer risk from residential area, park, and farmland was acceptable. Dermal contact accounted for the largest proportion of the overall exposure. It is recommended that a buffer zone be created between residential area and pollution sources using green spaces to block and adsorb PAHs. Sufficient space should be allocated to green spaces in cities to minimize the diffusion of pollutants when planning new industrial area and constructing roads.

Supplementary Information The online version contains supplementary material available at https://doi.org/10.1007/s11368-021-03050-6.

Funding This work was supported by the National Natural Science Foundation of China (Grant Nos. 41673107), Major project of Jiangsu Provincial Department of Education (20KJ, A170001) and National Water Pollution Control and Treatment Science and Technology Major Project (2017ZX07203-005).

References

Balgobin A, Singh NR (2019) Source apportionment and seasonal cancer risk of polycyclic aromatic hydrocarbons of sediments in a multi-use coastal environment containing a Ramsar wetland, for a Caribbean island. Sci Total Environ 664:474–486. https://doi.org/10.1016/j.scitotenv.2019.02.031

Cetin B (2016) Investigation of PAHs, PCBs and PCNs in soils around a heavily industrialized area in Kocaeli, Turkey: concentrations, distributions, sources and toxicological effects. Sci Total Environ 560–561:160–169. https://doi.org/10.1016/j.scitotenv.2016.04.037

China's Ministry of Environmental Protection (2009) National Standard of Chinese Soil Quality (GB15618–2009). http://www.doc88.com/p-3098747116486.html. Accessed 15 July 2009

Chen X, Wang YH, Cai ZC, Wu CB, Ye C (2020) Effects of land-use and land-cover change on nitrogen transport in northern Taihu basin, China during 1990–2017. Sustainability 12:3895. https://doi.org/10.3390/su12093895

Chen P, Liang J (2021) Polycyclic aromatic hydrocarbons in green space soils in Shanghai: source, distribution, and risk assessment. J Soil Sediment 21:967–977. https://doi.org/10.1007/s11368-020-02838-2

Chen X, Wang Y, Sun T, Chen Y, Ye C (2021) Evaluation and prediction of water quality in the dammed estuaries and rivers of Taihu Lake. Environ Sci Pollut Res. https://doi.org/10.1007/s11356-020-12063-6 Accessed 6 January 2021

Chang J, Zhang EL, Liu EF, Liu HJ, Yang XQ (2018) A 60-year historical record of polycyclic aromatic hydrocarbons (PAHs) pollution in lake sediment from Guangxi Province, Southern China. Anthropocene 24:51–60. https://doi.org/10.1016/j.ancene.2018.11.003

Crnković D, Ristić M, Jovanović A, Antonović D (2007) Levels of PAHs in the soils of Belgrade and its environs. Environ Monit Assess 125(1–3):75–83. https://doi.org/10.1007/s10661-006-9240-7

Dashtbozorg M, Bakhtiari AR, Shushizadeh MR, Taghavi L (2019) Quantitative evaluation of n-alkanes, PAHs, and petroleum biomarker accumulation in beach-stranded tar balls and coastal surface sediments in the Bushehr Province, Persian Gulf (Iran). Mar Pollut Bull 146:801–815. https://doi.org/10.1016/j.marpolbul.2019.07.023

Environmental Protection Department of Jiangsu Province (2007) Discharge standard of main water pollutants for municipal wastewater treatment plant & key industries of Taihu Area (BD32/1072–2007). https://wenku.baidu.com/view/6acb7ca0c850ad02df804151.html. Accessed 8 July 2007

Hadibarata T, Syafiuddin A, Ghfar AA (2019) Abundance and distribution of polycyclic aromatic hydrocarbons (PAHs) in sediments of the Mahakam River. Mar Pollut Bull 149:110650. https://doi.org/10.1016/j.marpolbul.2019.110650

He Y, He W, Yang C, Liu WX, Xu FL (2020) Spatiotemporal toxicity assessment of suspended particulate matter (SPM)-bound polycyclic aromatic hydrocarbons (PAHs) in Lake Chaohu, China: application of a source-based quantitative method. Sci Total Environ 727:138690. https://doi.org/10.1016/j.scitotenv.2020.138690

Huang YZ, Sui Q, Lyu SG, Wang JQ, Huang SX, Zhao WT, Wang B, Xu DJ, Kong M, Zhang YM, Yu G (2020) Tracking emission sources of PAHs in a region with pollution-intensive industries, Taihu Basin: From potential pollution sources to surface water. Environ Pollut 264:114674. https://doi.org/10.1016/j.envpol.2020.114674

Jia JP, Bi CJ, Guo X, Wang WP, Zhou XX, Chen ZL (2017) Characteristics, identification, and potential risk of polycyclic aromatic hydrocarbons in road dusts and agricultural soils from industrial sites in Shanghai, China. Environ Sci Pollut Res 24:605–615. https://doi.org/10.1007/s11356-016-7818-3

Katsoyiannis A, Breivik K (2014) Model-based evaluation of the use of polycyclic aromatic hydrocarbons molecular diagnostic ratios as a source identification tool. Environ Pollut 184:488–494. https://doi.org/10.1016/j.envpol.2013.09.028

Lei P, Zhang H, Shan B (2016) Vertical records of sedimentary PAHs and their freely dissolved fractions in pore water profiles from the northern bays of Taihu lake, Eastern China. RSC Adv 6(101):98835–98844. https://doi.org/10.1039/c6ra11180g

Lemieux CL, Long AS, Lambert IB, Lundstedt S, Tysklind M, White PA (2015) Cancer risk assessment of polycyclic aromatic hydrocarbon contaminated soils determined using bioassay-derived levels of benzo[a]pyrene equivalents. Environ Sci Technol 49(3):1797–1805. https://doi.org/10.1021/es504466b

Li J, Zheng Y, Luo X (2016) PAHs contamination in Beijing's topsoil: a unique indicator of the megacity's evolving energy consumption

and overall environmental quality. Sci Rep 6:33245. https://doi.org/10.1038/srep33245

Li QY, Wu JL, Zhao ZH (2018) Spatial and temporal distribution of polycyclic aromatic hydrocarbons (PAHs) in sediments from Poyang lake, China Plos One 13(10):e0205484. https://doi.org/10.1371/journal.pone.0205484

Li RF, Hua P, Cai JL, Wang X, Zhu Y, Huang ZY, Li PF, Wang ZY, Bai Y, Hu BX, Zhang J, Krebs P (2019a) A sixteen-year reduction in the concentrations of aquatic PAHs corresponding to source shifts in the Elbe River, Germany. J Clean Prod 223:631–640. https://doi.org/10.1016/j.jclepro.2019.03.159

Li AL, Der-Beek TA, Schubert M, Yu ZY, Schiedek T, Schueth C (2019b) Sedimentary archive of Polycyclic Aromatic Hydrocarbons and perylene sources in the northern part of Taihu Lake, China Environ Pollut 246(3):198–206. https://doi.org/10.1016/j.envpol.2018.11.112

Li Y, Liu M, Li RK, Sun P, Xia HB, He TH (2020a) Polycyclic aromatic hydrocarbons in the soils of the Yangtze River Delta Urban Agglomeration, China: Influence of land cover types and urbanization. Sci Total Environ 715. https://doi.org/10.1016/j.scitotenv.2020.137011

Li Q, Wu JL, Zhou JC, Sakievd K, Hofmanne D (2020b) Occurrence of polycyclic aromatic hydrocarbon (PAHs) in soils around two typical lakes in the western Tian Shan Mountains (Kyrgyzstan, Central Asia): Local burden or global distillation? Ecol Indic 108:105749. https://doi.org/10.1016/j.ecolind.2019.105749

Liu YG, Gao P, Su J, Silva EBD, Oliveria LMD, Townsend T, Xiang P, Ma LQ (2019) PAHs in urban soils of two Florida cities: background concentrations, distribution, and sources. Chemosphere 214(1):220–227. https://doi.org/10.1016/j.chemosphere.2018.09.119

Lu XZ, Gu AQ, Zhang YW, Chu XY, Hu XF (2020) Accumulation of pahs of the soils and assessment of their health risks at a village with plastic manufacturing in Taizhou, Zhejiang Province, Southeast China. J Soil Sediment 20(2):705–713. https://doi.org/10.1007/s11368-019-02425-0

Maliszewska-Kordybach B (1996) Polycyclic aromatic hydrocarbons in agricultural soils in Poland: preliminary proposals for criteria to evaluate the level of soil contamination. Appl Geochem 11:121–127. https://doi.org/10.1016/10.1016/0883-2927(95)00076-3

Mu XL (2016) Emission inventory of polycyclic aromatic hydrocarbons in China. Dissertation, China University of Petroleum

Nam JJ, Song BH, Eom KC, Lee SH, Smith A (2003) Distribution of polycyclic aromatic hydrocarbons in agricultural soils in South Korea. Chemosphere 50(10):1281–1289. https://doi.org/10.1016/S0045-6535(02)00764-6

Nisbet ICT, Lagoy PK (1992) Toxic equivalency factors (TEFs) for polycyclic aromatic hydrocarbons (PAHs). Regul Toxicol Pharma 16(3):290–300. https://doi.org/10.1016/0273-2300(92)90009-X

Obrist D, Zielinska B, Perlinger JA (2015) Accumulation of polycyclic aromatic hydrocarbons (PAHs) and oxygenated PAHs (OPAHs) in organic and mineral soil horizons from four U.S. remote forests. Chemosphere 134:98–105. https://doi.org/10.1016/j.chemosphere.2015.03.087

Paatero P, Tapper U (1994) Positive matrix factorization: a non-negative factor model with optimal utilization of error estimates of data values. Environmetrics 5(2):111–126. https://doi.org/10.1002/env.3170050203

Parra YJ, Oloyede OO, Pereira GM, Limaa PHAA, Caumoa SES, Morenikejib OA, Vasconcellosa PC (2019) Polycyclic aromatic hydrocarbons in soils and sediments in Southwest Nigeria. Environ Pollut 259:113732. https://doi.org/10.1016/j.envpol.2019.113732

Peng C, Chen WP, Liao XL, Wang ME, Ouyang ZY, Jiao WT, Bai Y (2011) Polycyclic aromatic hydrocarbons in urban soils of Beijing: status, sources, distribution and potential risk. Environ Pollut 159(3):802–808. https://doi.org/10.1016/j.envpol.2010.11.003

Qi HX, Chen XL, Du YE, Niu XJ, Guo F, Li WX (2019) Cancer risk assessment of soils contaminated by polycyclic aromatic hydrocarbons in Shanxi, China. Ecotox Environ Safe 182:109381. https://doi.org/10.1016/j.ecoenv.2019.109381

Samburova V, Zielinska B, Khlystov A (2017) Do 16 polycyclic aromatic hydrocarbons represent PAHs air toxicity? Toxics 5(3):17. https://doi.org/10.3390/toxics5030017

Semenov MY, Martinaite II, Golobokova LP, Khuriganova OI, Khodzher TV, Semenov YM (2017) Source apportionment of polycyclic aromatic hydrocarbons in Lake Baikal water and adjacent air layer. Chem Ecol 33(10):977–990. https://doi.org/10.1080/02757540.2017.1393533

Soltani N, Keshavarzi B, Moore F, Tavakol T, Lahijanzadeh RA, Jaafarzadeh N, Kermani M (2015) Ecological and human health hazards of heavy metals and polycyclic aromatic hydrocarbons (PAHs) in road dust of Isfahan metropolis, Iran. Sci Total Environ 505:712–723. https://doi.org/10.1016/j.scitotenv.2014.09.097

Sun JT, Pan LL, Tsang DCW, Zhan Y (2017) Organic contamination and remediation in the agricultural soils of China: A critical review. Sci Total Environ 615:724–740. https://doi.org/10.1016/j.scitotenv.2017.09.271

Wang JZ, Zhang K, Liang B, Zeng EY (2011) Occurrence, source apportionment and toxicity assessment of polycyclic aromatic hydrocarbons in surface sediments of Chaohu, one of the most polluted lakes in China. J Environ Monitor 13:3336. https://doi.org/10.1039/c1em10599j

Wang C, Zhou S, Wu S, Tang J, Li H, Du J (2020a) Exposure to polycyclic aromatic hydrocarbons (PAHs) in people living in urban and rural areas as revealed by hair analysis. Chemosphere 246:125764. https://doi.org/10.1016/j.chemosphere.2019.125764

Wang SB, Ji YQ, Zhao JB, Lin Y, Lin Z (2020b) Source apportionment and toxicity assessment of $PM_{2.5}$-bound PAHs in a typical iron-steel industry city in northeast China by PMF-ILCR. Sci Total Environ 713:136428. https://doi.org/10.1016/j.scitotenv.2019.136428

Wu QH, Leung JYS, Tam NFY, Chen SJ, Mai BX, Zhou XZ, Xia LH, Geng XH (2014) Biological risk and pollution history of polycyclic aromatic hydrocarbons (PAHs) in Nansha Mangrove, South China. Mar Pollut Bull 85(1):92–98. https://doi.org/10.1016/j.marpolbul.2014.06.014

Wuxi City Bureau of Statistics (2000–2018) Statistical yearbook of Wuxi City, China. http://tj.wuxi.gov.cn/ Accessed 2001–2019

Xia Z, Idowu I, Kerr E, Klaassen N, Assi H, Bray H, Marvin C, Thomas PJ, Stetefeld J, Tomy GT (2021) New approaches to reduce sample processing times for the determination of polycyclic aromatic compounds in environmental samples. Chemosphere 274:129738. https://doi.org/10.1016/j.chemosphere.2021.129738

Xu SS, Liu WX, Tao S (2006) Emission of polycyclic aromatic hydrocarbons in China. Environ Sci Technol 40(3):702–708. https://doi.org/10.1021/es0517062

Xu ZY, Wang CH, Li HX, Xu SD, Du J, Chen YJ, Ma C, Tang JH (2021) Concentration, distribution, source apportionment, and risk assessment of surrounding soil PAHs in industrial and rural areas: a comparative study. Ecol Indic 125:107513. https://doi.org/10.1016/j.ecolind.2021.107513

Yang XX, Ren D, Sun WW, Li XM, Huang B, Chen R, Lin C, Pan XJ (2015) Polycyclic aromatic hydrocarbons associated with total suspended particles and surface soils in Kunming, China: distribution, possible sources, and cancer risks. Environ Sci Pollut Res 22:6696–6712. https://doi.org/10.1007/s11356-014-3858-8

Yang J, Yang Y, Chen RS (2018) Modeling and evaluating spatial variation of polycyclic aromatic hydrocarbons in urban lake surface sediments in Shanghai. Environ Pollut 235:1–10. https://doi.org/10.1016/j.envpol.2017.12.032

Yang J, Qadeer A, Li M, Zhu JM, Huang YP, Du WN, Wei XY (2019) Occurrence, source, and partition of PAHs, PCBs, and OCPs in

the multiphase system of an urban lake, Shanghai. Appl Geochem 106:17–25. https://doi.org/10.1016/j.apgeochem.2019.04.023

Yang J, Sun P, Zhang X, Wei XY, Huang YP, Du WN, Qadeer A, Liu M, Huang Y (2021) Source apportionment of PAHs in roadside agricultural soils of a megacity using positive matrix factorization receptor model and compound-specific carbon isotope analysis. J Hazard Mater 403:123592. https://doi.org/10.1016/j.jhazmat.2020.123592

Yin HL, Guo LL, Xiao MW, Peng P, Bai J (2015) Combination of Unmix and positive matrix factorization model identifying contributions to carcinogenicity and mutagenicity for polycyclic aromatic hydrocarbons sources in Liaohe delta reed wetland soils, China Chemosphere 120:431–437. https://doi.org/10.1016/j.chemosphere.2014.08.048

Zhang YX, Shen HZ, Shu T, Ma JM (2011) Modeling the atmospheric transport and outflow of polycyclic aromatic hydrocarbons emitted from China. Atmos Environ 45(17):2820–2827. https://doi.org/10.1016/j.atmosenv.2011.03.006

Zhang MM, He P, Qiao G, Wang JW, Huang JT, Yuan XT, Li Q (2019) Distribution, sources, and risk assessment of polycyclic aromatic hydrocarbons (PAHs) in surface sediments of the Subei Shoal, China Mar Pollut Bull 149:110640. https://doi.org/10.1016/j.marpolbul.2019.110640

Zheng SS, Wang PF, Wang C, Hou J (2015) Sediment resuspension under action of wind in Taihu Lake, China Int J Sediment Res 30(1):48–62. https://doi.org/10.1016/S1001-6279(15)60005-1

Zheng H, Yang D, Hu TP, Li Y, Zhu GH (2017) Source apportionment of polycyclic aromatic carbons (PAHs) in sediment core from Honghu Lake, Central China: comparison study of three receptor models. Environ Sci Pollut Res 24:25899–25911. https://doi.org/10.1007/s11356-017-0185-x

Zheng H, Xing XL, Hu TP, Zhang Y, Zhang JQ, Zhu GH, Li Y, Qi SH (2018) Biomass burning contributed most to the human cancer risk exposed to the soil-bound PAHs from Chengdu Economic Region, Western China. Ecotox Environ Safe 159:63–70. https://doi.org/10.1016/j.ecoenv.2018.04.065

Zheng HJ, Kang SC, Chen PF, Li QL, Tripathee L, Maharjan L, Guo JM, Zhang QG, Santos E (2020) Sources and spatio-temporal distribution of aerosol polycyclic aromatic hydrocarbons throughout the Tibetan Plateau. Environ Pollut 261:114144. https://doi.org/10.1016/j.envpol.2020.114144

Zhong JC, Yu JH, Wa JJ, Liu DH, Chen CC, Fan CX (2020) The co-regulation of nitrate and temperature on denitrification at the sediment-water interface in the algae-dominated ecosystem of Lake Taihu, China. J Soil Sediment 20:2277–2288. https://doi.org/10.1007/s11368-019-02558-2

Zong RX, Chen JY, Wang YT, Xing Z, Wei W, Yu J (2019) Characteristics and influencing factors of polycyclic aromatic hydrocarbons in surface soils from typical industrial areas of Chengdu. Environ Sci 40(10):4594–4603. https://doi.org/10.13227/j.hjkx.201903088